JOURNAL OF CATALYSIS 113, 383–397 (1988)

Carbon Deposition on Platinum during Ethylene Oxidation

N. L. WU AND J. PHILLIPS[1]

Department of Chemical Engineering, The Pennsylvania State University, University Park, Pennsylvania 16802

Received September 22, 1987; revised March 29, 1988

It was found that the structures of carbon films which formed on platinum foil surfaces under ethylene oxidation-fuel excess conditions were a function of temperature. In ethylene-only atmospheres (no oxygen), films formed only above 870 K and were partially graphitic and partially turbostratic. In addition, the films were preferentially oriented with graphite basal planes parallel to the foil surface. Under reaction conditions between 770 and 960 K initially only an amorphous film formed, but after a lengthy treatment a large number of fibers and fibrous shells formed. This was postulated to result from the action of small platinum particles, produced independently by a catalytic etching process. These particles were present only over this limited temperature range. Above 960 K under reaction conditions, preferentially oriented graphitic films formed on the surface. Under all conditions an unusual form of carbon, chaoite, was found to be present in the carbon films.

INTRODUCTION

Carbon deposition on metals is a process which has drawn widespread attention (*1–3*). It is studied for a variety of reasons including its connection to the deactivation of metal catalysts, possible degradation of the properties of reactor wall materials (*4*), and as a possible source for future production of graphitic fibers. Previous studies (*5*, *6*) of the structure of carbon deposits on noble metals have been carried out at very high temperatures (>1000°C) with one exception (*7*) and the carbon has been deposited via the decomposition of a single hydrocarbon species. In brief, previous work with noble metals has not involved reacting gas mixtures. Yet, recent work on other Group VIII metals such as iron and nickel indicates that the structure of the carbon surface deposits is a function of temperature and the composition of the gas phase (*1*, *8–11*). Indeed, in recent work (*12*, *13*) carbon was observed to deposit on platinum foils under ethylene oxidation conditions ($C_2H_4 + O_2$ mixtures) at temperatures as low as 500° C. Moreover, the structure of the carbon which deposited was found to be sensitive to reaction parameters such as temperature and gas composition, although details were not provided.

This paper is a report on a detailed analysis of the carbon structures which form on platinum foils under ethylene oxidation conditions. The characterization was conducted using primarily transmission electron microscopy (TEM) and energy-dispersive X-ray analysis (EDX). In brief, the following were observed: Three types of carbon layers were found on the foil surfaces following treatments under reaction conditions, and each type occurred only under a well-defined range of reaction conditions. The conditions under which different structures formed were (i) ethylene (2%) plus N_2 (98%) at temperatures above about 870 K, (ii) fuel-rich $O_2 + C_2H_4$ reaction mixtures at temperatures between 770 and 960 K, and (iii) fuel-rich reaction mixtures above 960 K. Following treatments in C_2H_4 and nitrogen (condition (i)) sheets of turbostratic and graphitic carbon were formed. Treatments under reaction conditions at less than 960 K (condition (ii))

[1] To whom correspondence should be addressed.

0021-9517/88 $3.00

resulted in the formation of complex structures in which several forms of carbon were present including graphitic fibers and amorphous, nonoriented carbon. It is noted that, under condition (ii) "catalytic etching" of platinum foils, and the consequent formation of platinum particles at the surface, was previously observed (*12*, *13*). It is postulated that under these conditions the platinum particles catalyze the conversion of some amorphous carbon into graphitic carbon. This is postulated to occur both through a fiber growth mechanism, which must be similar to that observed for fiber growth from particles made from a variety of metals, and via a process akin to nucleation of crystals from a supersaturated solution. A nucleation process similar to that observed here was seen for palladium particles deposited on amorphous carbon (*14*). At higher temperatures under reaction conditions (condition (iii)) a layered, essentially graphitic structure formed. It must also be noted that under all the conditions listed above an unusual crystal form of carbon, chaoite (*15*), was also found to be present.

EXPERIMENT

In this work polycrystalline platinum foil samples (99.99% purity; Goodfellow Metals, Ltd.) were treated in a quartz reactor, described in detail elsewhere (*12*), under a variety of controlled reaction conditions and subsequently examined with a scanning electron microscope (SEM, ISI SUPER IIIA) or scanning transmission electron microscope (STEM, Philips 420).

The reactor was attached to a high-vacuum/gas-handling system, such that a pressure of 1×10^{-5} Torr was generally achieved during the annealing step. However, under actual flow conditions the system was always operated at approximately 1 atm.

Gases used in this experiment were research grade and were further purified whenever possible. For example, oxygen was further purified by passing through a cooled 5-Å molecular sieve trap. Nitrogen was passed first through a heated copper turning trap and then through a cooled molecular sieve trap. Ethylene of 99.98% purity (Matheson) was used as received. Total gas flow was maintained at 300 cm^3/min (10 cm/s over the sample) during all experiments. Composition of the gas was controlled with calibrated rotameters.

Prior to performing controlled atmosphere treatments, each foil sample was activated following a standard procedure, described in detail elsewhere (*12*). The pretreatment procedure used in this work is similar to that used by other workers (*16–18*), who found that a high-temperature calcining step is required to "activate" platinum foils. Other workers have reported that Auger studies indicate that treating platinum at high temperatures in oxygen removes most impurities leaving a clean platinum surface (*19*, *20*).

Once the final gas mixture was introduced experimental conditions were maintained for 40 to 70 h, in most cases. At the end of each experiment the samples were cooled rapidly (ca. 20 min) to room temperature in flowing nitrogen. After removal from the reactor the samples were examined in an SEM and/or STEM. Thick carbon deposits were removed from the samples for further study by dissolving the platinum foil in aqua regia. This unavoidably resulted in the dissolution of some of the platinum particles in the carbon film itself. Energy-dispersive X-ray analysis and selected area diffraction (SAD) were used for chemical and structural analyses of the isolated surface structures.

RESULTS

In a previous study (*12*) it was shown that under reaction conditions carbon deposits only on platinum foils under a limited range of conditions. It was shown, for example, that carbon is never deposited under oxygen excess conditions ($O_2 : C_2H_4 > 3 : 1$), presumably because any carbon which is deposited under these conditions is rapidly

burned off. At temperatures less than approximately 770 K, even under fuel excess conditions, carbon is not deposited. Indeed, on the basis of the carbon structures which form, three distinct "regions" can be identified: Region I, ethylene (2%), nitrogen mixture above about 870 K in which oxygen is carefully excluded; Region II, fuel excess between approximately 770 and 960 K; and Region III, fuel excess above 960 K. A detailed description of the structure of the carbon layer which forms in each of these regions is given below.

Region I. Carbon deposition in ethylene (2% in N_2) at 873 K or above produces layers consisting of two major structures. They are graphitic platelets and "stripes" of apparently less-ordered carbon (Figs. 1a and 1b). The latter are found to have a maximum width around 0.5 μm and are all oriented parallel to each other in a direction which is very possibly a function of the underlying platinum grain structure. Indeed, close observation of Fig. 1b clearly indicates that there is a preferential pattern to the growth of both of the carbon structures. That is, many of them appear to grow outward from a common starting line. Thus, they are irregular on one end and rather neatly "cut-off" on the other end. The formation of this pattern is possibly related to the underlying hill-and-valley platinum facets (see Ref. (*12*)). That is, the stripes seem to lie along the tops of major facets (low index planes), beginning and ending at major "steps." The platelets also seem to grow along major facets, but are apparently widest at the point where the facet intersects a major step. This apparent preferential orientation is further confirmed by diffraction data, as discussed below.

The crystallinity of the film was determined by using microprobe SAD (MSAD). In all cases, MSAD from the platelets yields a [001] spotty ring pattern, indicating a highly graphitized structure. The average (graphite) crystal size, L_a (see Table 1), is ~300 Å. On the other hand, MSAD of the stripes yields only diffuse (hk0) rings, characteristic of a turbostratic carbon structure (*21*). Moreover, the absence of [00l] reflections in both cases indicates that the graphite crystallites in both structures grow preferentially with their basal planes parallel to the metal surface. In addition to these graphitic carbon structures, a small amount of chaoite (*15*), also known as "white carbon," was also observed.

Region II. The rate of carbon formation is highest under Region II conditions (*12*). It is also important to note that the temperature at which carbon deposition starts is very sharply defined. A very thick carbon layer is found following treatment at 770 K, whereas no carbon at all is formed at 750 K. TEM studies of the full developed (40-h)

TABLE 1

Carbon Deposition: Reaction Condition and Carbon Structures

Reaction condition	Carbon structure	Classification[c] of the carbon structures
2% C_2H_4/98% N_2	Graphite platelet (major)	I
$T > 870$ K	(L_a = 300 Å)[a]	
(Region I)	Turbostratic carbon (major)	I
	Chaoite (minor)	III
$O_2/C_2H_4 < 3.0$	Turbostratic carbon	I
770 K $< T <$ 960 K	(major)	
(Region II)	Fibrous carbon (major)	II
	(L_c = 40 Å)[b]	
	Pt-containing particles (major)	
	Chaoite (minor)	III
$O_2/C_2H_4 < 3.0$	Graphitic layer with	I
$T <$ 960 K	hexagonal pits (major)	
(Region III)	(L_a = 400 Å)	
	Ill-defined fiber-like carbon (minor)	II
	(L_c = 100 Å)	
	Chaoite (minor)	III

[a] L_a, average graphite crystal size measured along the basal graphite plane. This number is calculated using the Debye–Sherrer equation based on the linewidth of the graphite (100) reflection.

[b] L_c, average graphite crystal size measured along the c-axis of the graphite structure. This number is based on the linewidth of the graphite (002) reflection.

[c] The carbon structures formed under different reaction conditions are categorized into three groups in order to facilitate the discussion. They are (I) lamellar, continuous carbon thin films consisting of graphite crystallites with basal planes preferentially oriented parallel to the metal surface; (II) fibrous carbon; and (III) chaoite.

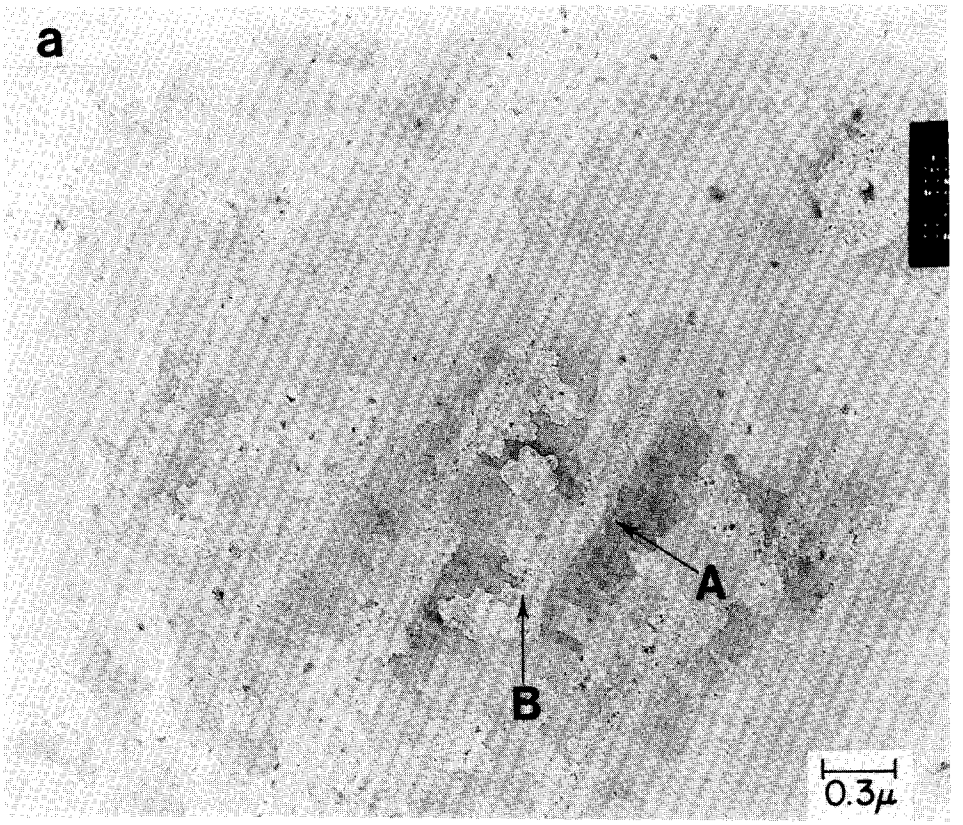
a
A
B
0.3μ

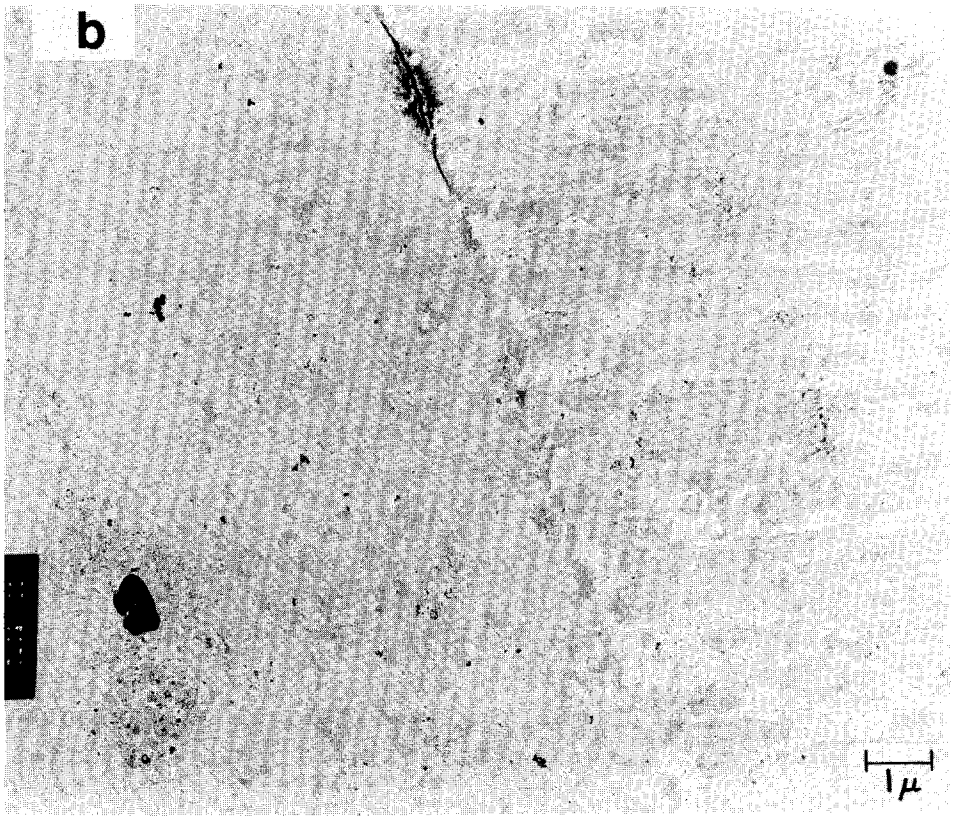
b
1μ

carbon layers formed under Region II conditions show three major features: (i) electron-opaque particles, (ii) cross-linked (fibrous) carbon, and (iii) (turbostratic) thin carbon layers (Fig. 2a). As described in an earlier publication (*12*), EDX, SAD, and dark-field (DF) analyses indicate that the opaque particles consist of an inner core of platinum single crystal totally encapsulated by a thin fibrous carbon layer. It was found that the graphite basal planes of the fibers were oriented parallel to the shell surfaces. In examining the figures it must be noted that some of the platinum particles in the shells and at the fiber tips were unavoidably dissolved during the sample preparation.

Fibrous carbon. MSADs from segments of the cross-linked carbon features give, in addition to (hk0) diffuse rings, (00l) arcs (Fig. 2c). Recording the image of the segments shown at the central spot of an underfocused diffraction pattern (Fig. 2c) shows that the central line between the (00l) arcs is parallel to the central axis of the fiber, indicating that the fiber contains graphite basal planes and these graphite planes are parallel to the fiber long axes. The DF image using the graphite (002) reflection shows that the (00l) rings appearing in the large-area SAD pattern come only from these fibers (Fig. 2b). The *d*-spacing of the (002) planes in the fibers is 3.40 Å and the crystal size, L_c (see Table 1), is ~40 Å. These data are similar to those of the carbon fibers reported elsewhere (*22*). Analysis also shows that the outer carbon shells of the large platinum-containing particles have structures similar to those of the cross-linked fibers.

Thin carbon layer. Thin carbon layers (relatively electron transparent) are found surrounding the fibrous carbon structures (Fig, 2a). MSAD from these regions results in only diffuse (hk0) rings characteristic of turbostratic carbon structures. As in Region I, the lack of (00l) reflections indicates preferential orientation parallel to the metal surface. The average crystal size, L_a, is about 40 Å.

The evolution of the three major features formed in Region II was determined by studying the development of the carbon surface layer as a function of the period of treatment (Fig. 3). For example, after a 3-h treatment at 860 K in 1.5 : 1 $O_2 : C_2H_4$, a continuous turbostratic carbon layer formed (Fig. 3a). At this stage, the platinum-containing particles were found to be more or less evenly distributed over the entire film and to have a maximum size no larger than 100 Å. A low density of fiber-like structures was also observed, but there was little branching of these fibers. As the reaction periods were increased to 6 and 30 h (Figs. 3b and 3c), platinum-containing particles were found in clusters. Also, both the maximum size and the density of platinum particles apparently increased with time. Furthermore, carbon layers in the vicinity of platinum particle clusters appear distinctly darker than regions without particles, indicating that more closely packed carbon structures form in the particle region.

Formation of cross-linked carbon fibers was observed after 6 h of deposition (Fig. 3b). The fibrous carbon structures observed after a 6-h treatment consist of much better-defined sheathes than those observed after a 3-h deposition (Fig. 3a). Moreover, these fibers appear to grow preferentially at positions where a large quantity of small platinum particles are present. That is, the density of the small particles within and/or along these fibrous branches is much higher than that within the turbostratic carbon region. In fact, after prolonged (>30 h) deposition (Figs. 2a and 3c), almost all the platinum-containing particles are associated with the fibers or fibrous shells. More-

FIG. 1. Carbon deposition in Region I. (a–b) TEM micrographs of the carbon layers formed on platinum following treatment for 40 h in 2% C_2H_4 + N_2 at 873 K. Shown are graphitic platelets (A) and oriented turbostratic "stripes" (B).

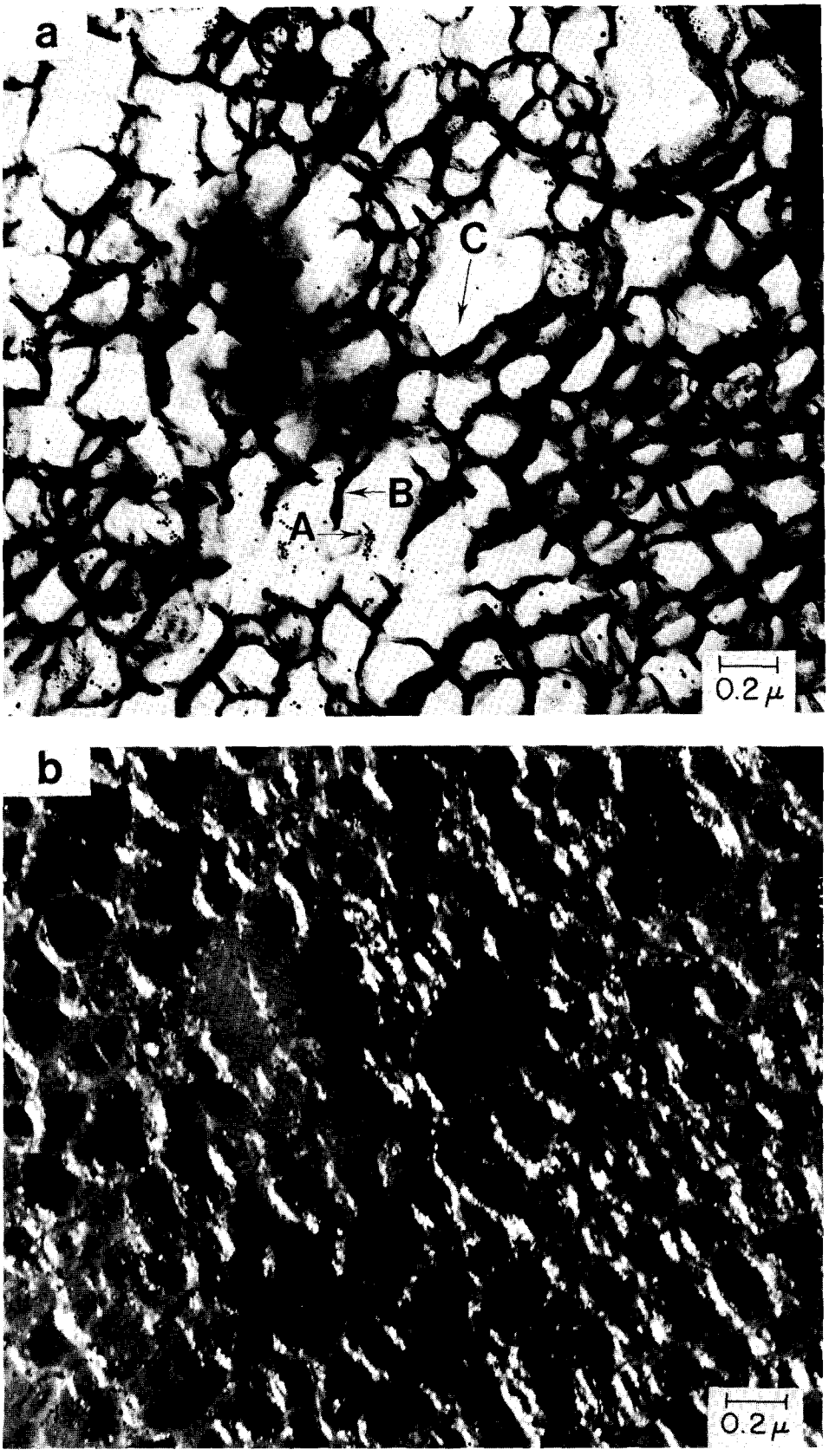
a
C
B
A
0.2 μ
b
0.2 μ

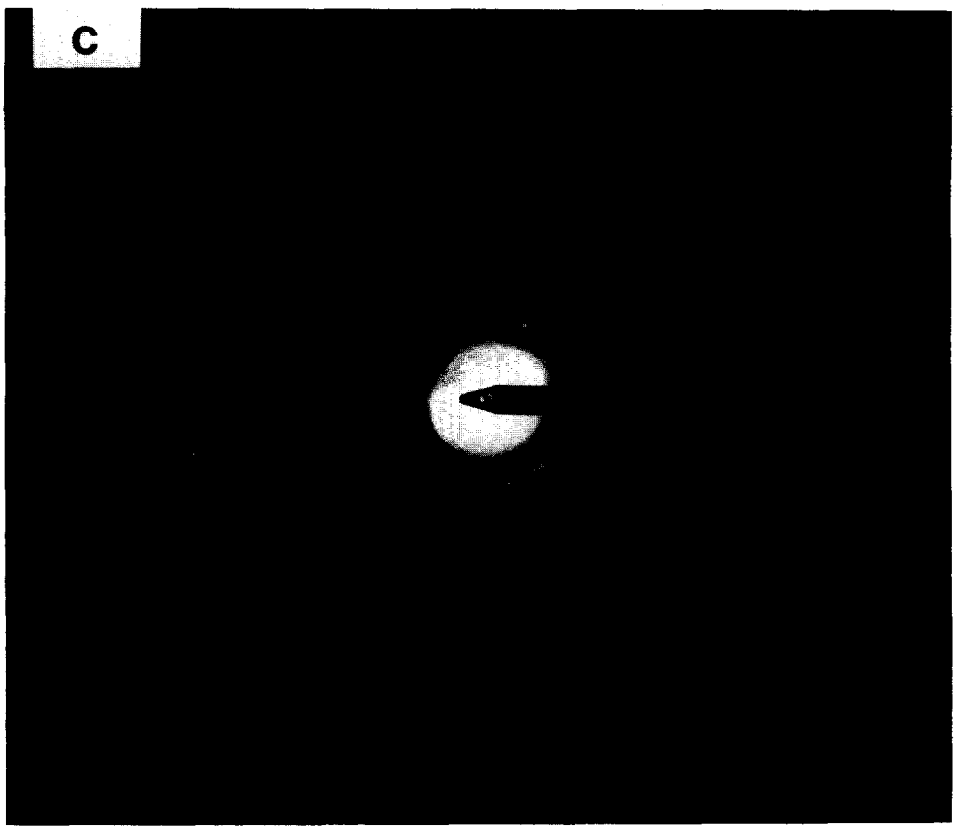

FIG. 2. Carbon deposition in Region II. (a) TEM micrograph of a carbon film formed after 40 h of treatment at $T = 860$ K in a fuel excess O_2/C_2H_4 mixture. Shown are (A) platinum particles, (B) fibrous carbon, and (C) turbostratic carbon. (b) Dark-field image of (a) obtained from graphite [002] reflection. Close inspection shows all bright areas in this picture arise from fibers seen in (a). (c) MSAD of fibrous carbon (B). Note, the fiber "image" seen in the center is parallel to the arcs in the diffraction pattern.

over, the fibers and shells clearly become thicker with time. It must also be noted that the particles clearly are not randomly placed on the surface, but rather are found clustered in the fiber regions. Large areas of amorphous carbon are particle and fiber free.

Region III. Treatment under reaction conditions at temperatures above 960 K produces primarily a continuous carbon thin film and a low density of short-ranged fiber-like carbon structures (Figs. 4a and 4b). No platinum-containing particles or even empty carbon shells are found. On the continuous carbon films there are areas showing shallow, apparently hexagonal, pits (Figs. 4a and 4b). MSAD from the areas containing the hexagonal produced exclusively (00l) spot patterns, and analysis indicated that the average crystal size, L_a, is around 400 Å.

The fiber-like structures formed in Region III are primarily short-ranged and the sheaths of these fibers are not as well-defined as those shown on the fully developed fibers formed in Region II (Fig. 2a). In fact, they are rather similar to the unbranched fibers formed at the earliest stage (3 h) of the deposition in Region II (Fig. 3a). MSAD and DF analyses show that the (00l) rings which appear in the large-area SAD pattern come solely from the fibrous struc-

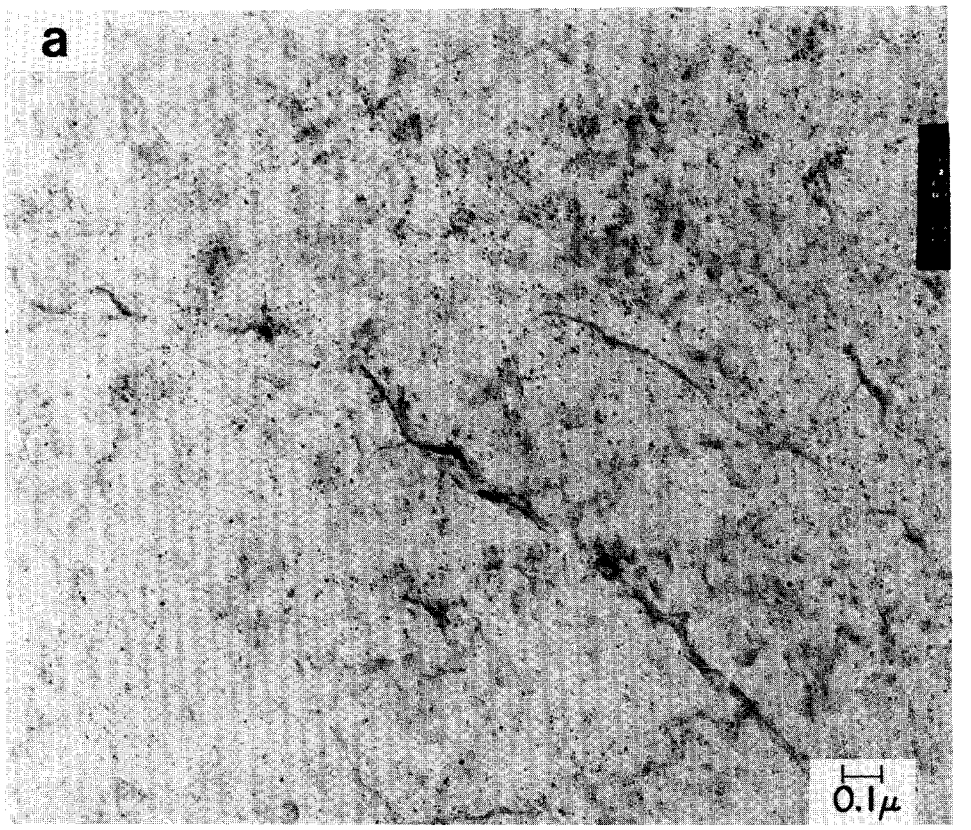
a
0.1μ

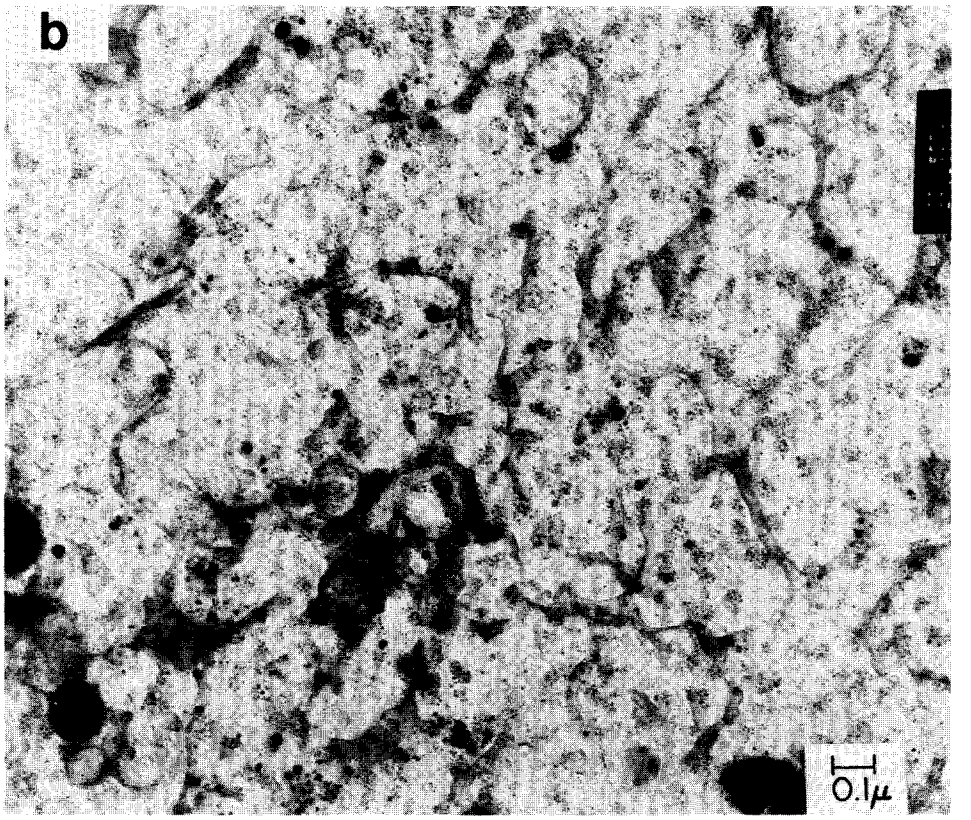
b
0.1μ

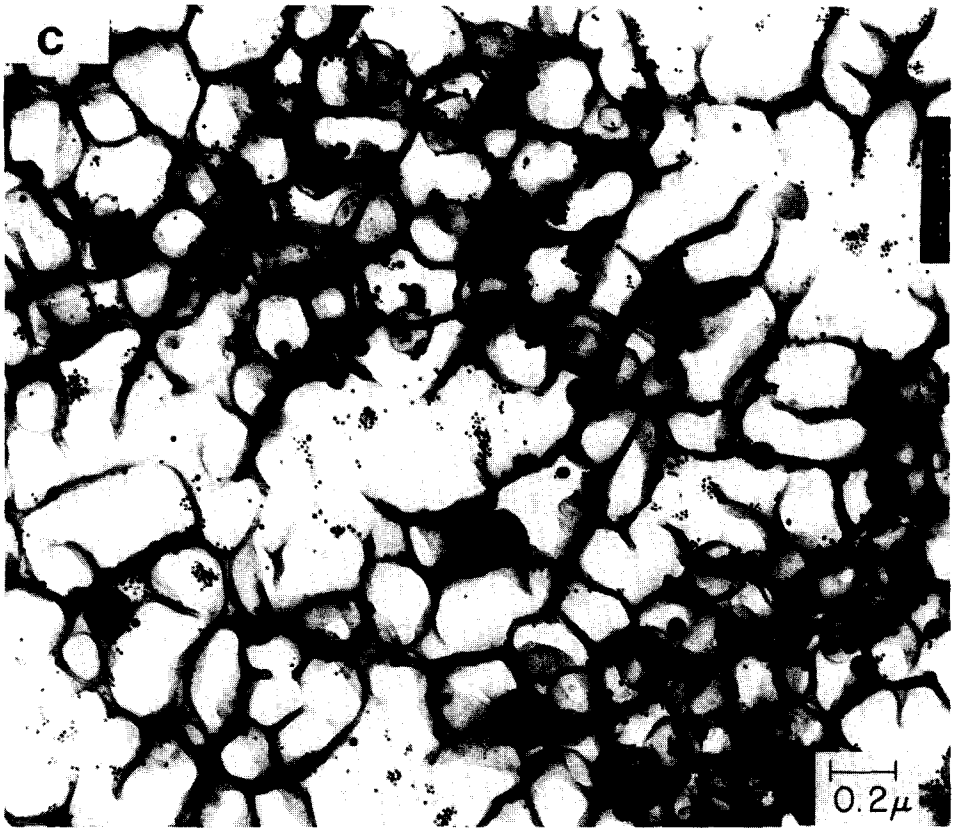

FIG. 3. Dynamics of carbon deposition in Region II. Shown are TEM micrographs of carbon films formed on platinum following treatment at $T = 860$ K in a 1.5 : 1 O_2 : C_2H_4 mixture after (a) 3 h, (b) 6 h, (c) 30 h.

tures. The average crystal size, L_c, is about 100 Å, which is more than two times larger than that of the branched fibers formed at low temperatures.

Chaoite. In addition to the graphitic form of carbon described above, an allotropic form of carbon, chaoite (*22, 23*), is also observed under all the deposition conditions discussed above.

All the chaoite formed during C_2H_4 treatments is in the form of large single crystals with well-defined, faceted outlines (Fig. 5a). SAD of these crystals gives clear six-fold spot patterns, which are usually superimposed by (00l) graphite rings (Fig. 5b). EDX of these crystals shows no signals other than those of Cu, which can be ascribed to the mounting grid material. (Since EDX is insensitive to elements with a z number below 11, carbon will not be detected.) This analysis indicates that the diffraction pattern is not associated with any Si or Al compounds/impurities as speculated by some earlier workers (*24*).

DISCUSSION

Lamellar carbon thin film. Basically, there are three types of carbon microstructures observed in this study (Table 1). They are (i) continuous, lamellar, partially graphitized, carbon thin films; (ii) fibrous carbon; and (iii) chaoite.

The continuous, lamellar carbon films containing graphitic crystallites with their basal planes parallel to the metal surfaces have been found under all deposition condi-

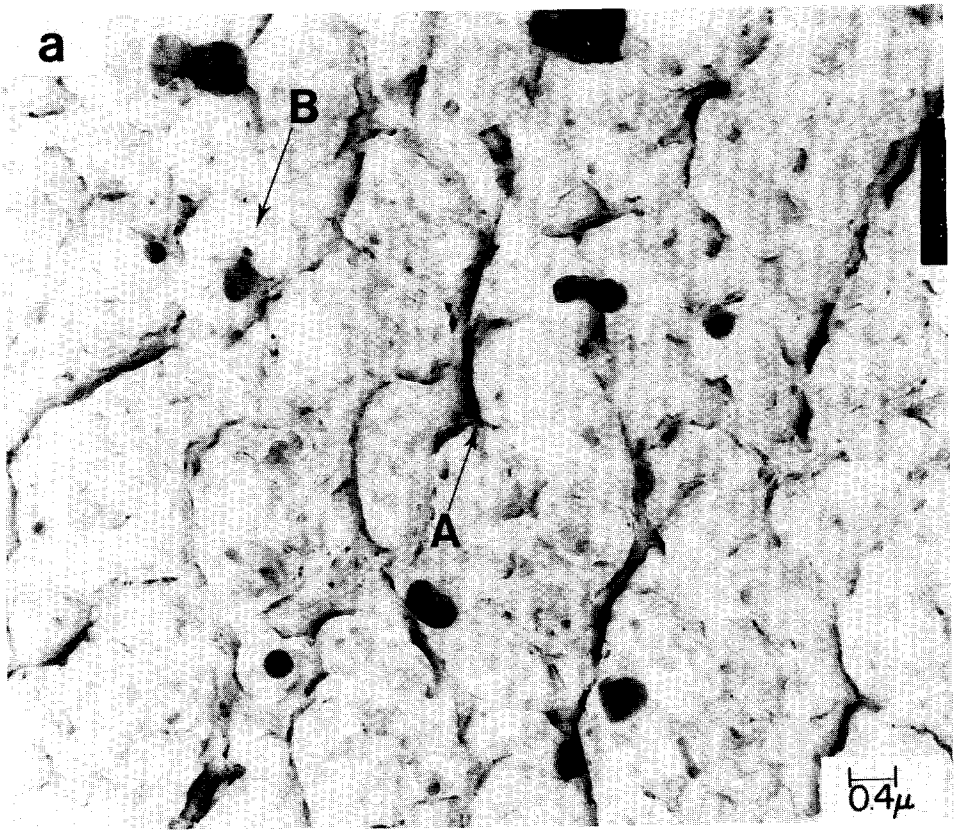
a
B
A
0.4μ

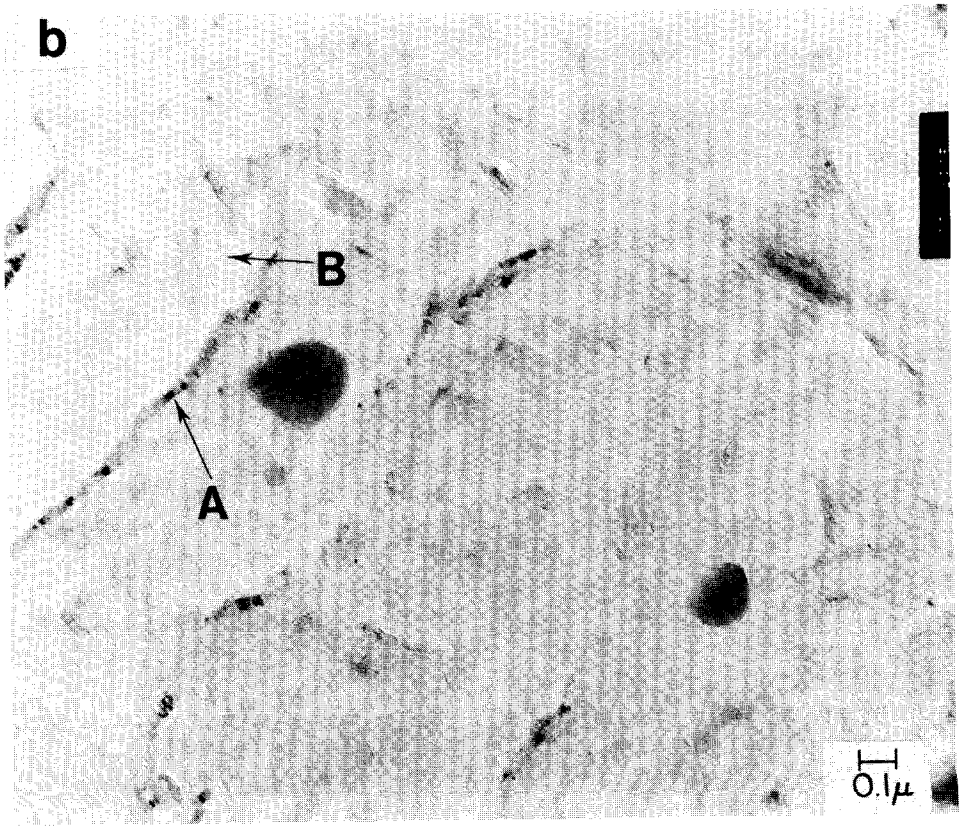
b
B
A
0.1μ

tions (Table 1). However, these films vary greatly in their degree of graphitization, as indicated by the range of observed graphite crystal sizes, L_a. For example, the lamellar films formed in Region II are primarily turbostratic while those formed in Region III are almost completely graphitized. Thin films formed in the ethylene treatments contain both turbostratic and graphitized lamellar carbon structures. These observations can best be explained by a model which assumes that the degree of graphitization of the films is a result of the competition between the crystal ordering process and the carbon deposition process (*25, 26*). That is, it is assumed that in those instances in which film formation is slow, surface carbon atoms will have enough time to diffuse along the surface and attach to the existing graphitic domains, before they collide with and become "trapped" by other free carbon atoms and/or small clusters. In such cases the existing graphitic domains can grow continuously and highly graphitized thin films will form. In contrast, if the carbon deposition is very fast, the probability of collisions among the free carbon atoms increases. This results in an increase in the formation of new graphite nuclei and/or less-ordered carbon clusters. Thus, in this case, the growth of the existing graphite domains is limited, and a less-ordered carbon layer is most likely to be formed. Aspects of the above model are similar to one proposed by Tesner and Refalkes (*27*), although in that work deposition was by thermal (not reactive) decomposition of hydrocarbons.

This model is consistent with the results observed in this study. For example, the carbon deposition is fastest in Region II; hence the lamellar carbon films formed under these deposition conditions have the smallest (average) graphite crystal size, and most of the carbon in the film is turbostratic (Table 1). On the other hand, the carbon films formed in Region III have the largest average (graphite) crystal size because (i) the rate of carbon deposition is comparable to that in ethylene treatment and much lower than that in Region II, and (ii) the films are formed at higher temperatures, which results in an increase in the diffusity of the carbon atoms, and hence the ordering process.

The formation of the hexagonal pits on the lamellar carbon films formed in Region III (Fig. 4) can be ascribed to the preferential combustion of the carbon atoms by oxygen at the grain boundaries of an ensemble of graphite domains. Similar morphologies have been frequently reported in the earlier studies of the graphite oxidation processes (*28*).

Fibrous carbon. Fibrous carbon is primarily formed in Region II (Fig. 2) where platinum-containing particles are also formed. It is clear that the fibers observed in this work are very similar in structure to those observed by previous workers (*7, 29–31*) to form behind metal particles during the catalytic decomposition of various carbon-containing molecules.

Any model of the formation of the fibrous carbon structures must account for the following observations: (i) most of the fibrous carbon is formed after a continuous lamellar turbostratic carbon film is first formed on the platinum surface, (ii) the fibrous structures are always associated with one or more small platinum particles, (iii) the fibers thicken with time, and (iv) surrounding large platinum particles are graphitized carbon shells. Previous models of the growth of fibers during the pyrolosis of various hydrocarbons on iron, cobalt, and nickel particles clearly explain most of the

FIG. 4. Carbon deposition in Region III. (a–b) TEM micrographs of carbon layer formed on platinum following 40 h of treatment in a fuel excess $O_2 : C_2H_4$ mixture at 1000 K. Shown are (A) fibrous carbon and (B) hexagonal pits. (The hexagonal pits are shallow and difficult to see.)

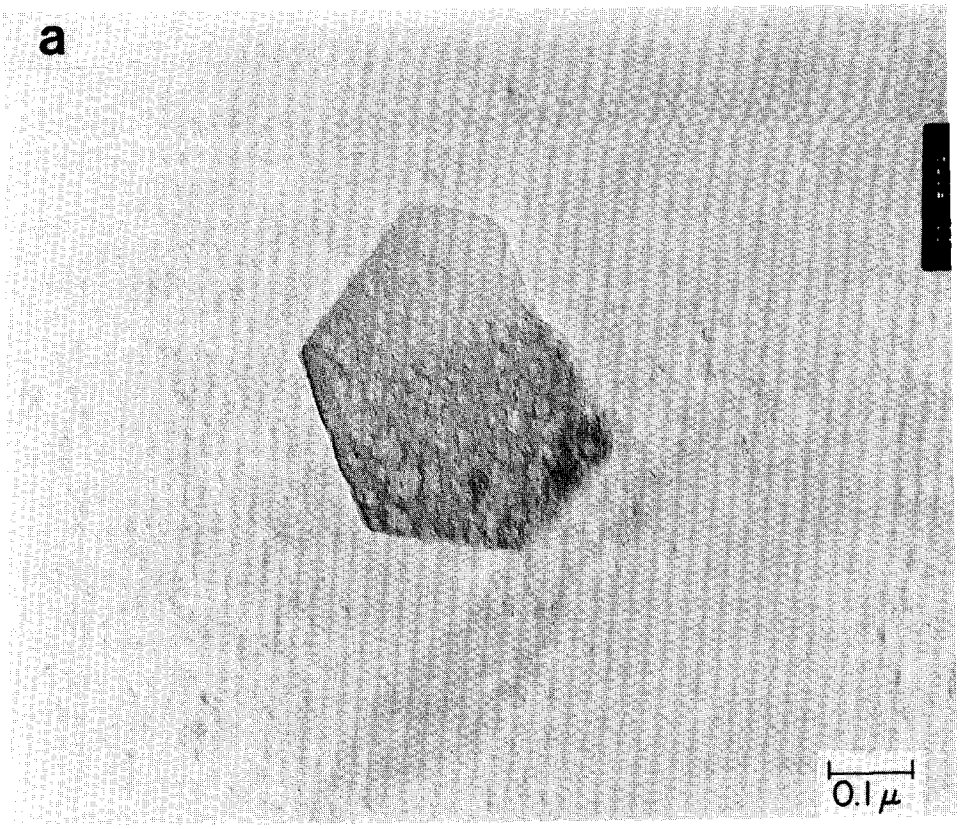
a
0.1 μ

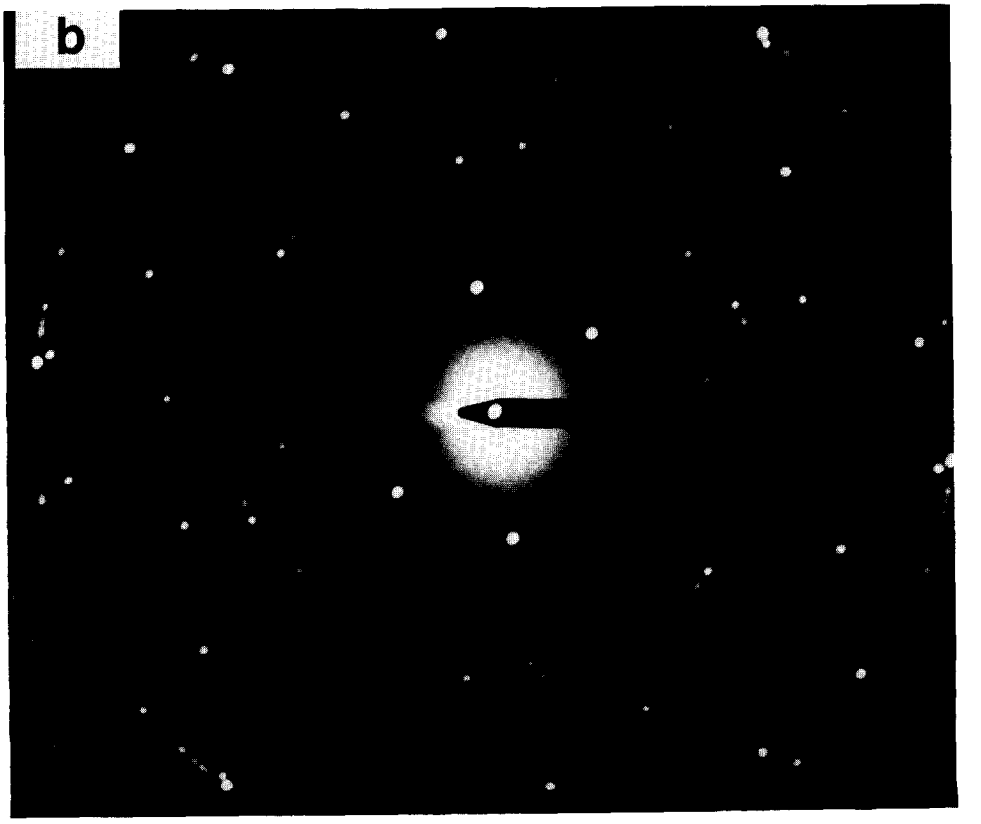
b

observations made in this study. Various workers have suggested that fibers are produced by small metal particles via a process of carbon diffusion through and then excretion from the particles with the driving force being thermal or concentration gradients (*1, 29, 32, 33*). Although this model was primarily developed to explain fiber formation from iron and nickel particles, it applies in this case as well because carbon is known to rapidly diffuse through platinum (*34*). Previously it has always been assumed that hydrocarbons adsorbed from the gas onto the metal particle surface are the source of carbon. In this case the amorphous carbon layer is assumed to be the source of the carbon. There is precedent for this suggestion as it has previously been shown that palladium particles will catalyze the conversion of an amorphous carbon layer into graphite (*14*). Another possibly applicable model is that adsorbed hydrocarbons decompose and/or react with the metal. This is followed by diffusion of a surface species to a graphitic interface where carbon atoms are added to a growing crystal (*35*).

The above models can explain the observed fiber growth, but not the complete encapsulation of the larger platinum particles. It is suggested that a phenomenon which is best described as a nucleation and growth from a supersaturated solution takes place around all the platinum particles. That is, the platinum surface is a heterogeneous site, capable of nucleating graphitic structures. These structures then continue to grow by the slow addition of atoms from the surrounding amorphous material. This is consistent with the observed graphitic platelet growth in Regions I and II. It is also consistent with the observation that the fibers appear to thicken with time, a phenomenon observed elsewhere as well (*30*). The reason that small particles tend to "grow" fibers and large particles do not is probably that the small thermal and/or concentration gradients which develop across a particle during the initial graphitization are too small to move the larger particles.

One major difference between platinum and other metals is the supposed origin of the fiber producing small particles. In general with iron and nickel it is assumed that the small particles are produced from larger structures when stresses produced by the formation of metal carbides or subsurface graphite become large enough to "lift out" particles (*36*). In contrast, in this case it is suggested that the metal particles which produce the fibers are created by a totally independent process, catalytic etching.

One other related observation which requires comment is the finding that carbon deposition under reaction conditions begins at a much lower temperature (~770 K) than that of carbon deposition in a nonreaction environment in which the ethylene concentration is just as high (~870 K). It is suggested that under reaction conditions unstable radical species are present in the gas phase. Some of these radicals are responsible for the observed catalytic etching (*12, 13*). Other radical species are likely responsible for the enhanced carbon deposition rate. This suggestion is consistent with earlier observations of low-temperature homogeneous ethylene oxidation kinetics (*37*) as well as the current understanding of the mechanism of homogeneous ethylene oxidation (*38, 39*). It is also consistent with the observation that some gas-phase radical-initiated processes, such as some types of soot formation, occur only over a limited temperature range (*40*). In related work (*41*), it has been shown that the rate of carbon deposition on a solid surface during

FIG. 5. Chaoite. (a) TEM micrograph of a chaoite crystal formed in Region I. (b) SAD of the crystal shown in (a).

hydrocarbon pyrolysis is a strong function of the gas-phase radical concentration.

In summary, it is postulated that the small platinum particles which form as a result of catalytic etching catalyze the conversion of amorphous carbon to fiber-like structures, whereas the large platinum particles are immobile, converting only platinum in their immediate vicinity, resulting in the formation of graphitic shells.

Chaoite. While chaoite (*42, 43*) has previously been artificially formed only at temperatures above 2000 K (*15, 23, 44*), other types of carbynes have been formed at temperatures below 800 K (*45–47*), but only in the presence of catalysts such as Si, Al, Co, and Mn. By analogy, it is possible that the platinum surface may catalyze the formation of chaoite.

SUMMARY

Carbon deposition on platinum is observed when platinum foils are treated either in ethylene (Region I) or in the O_2 + C_2H_4 mixtures at temperatures higher than 770 K (Region II and Region III). Ethylene treatment produces continuous, lamellar carbon thin films consisting of graphitic platelets and stripes of turbostratic carbon layers. No platinum reconstruction occurs during the carbon deposition and the platinum surface remains faceted.

The structure of the carbon layer formed in the O_2 + C_2H_4 mixtures is found to be a function of temperature and the duration of the treatment. At $T < 960$ K (Region II), carbon deposition first produced a continuous turbostratic carbon layer and evenly distributed platinum particles. This is followed by the formation of cross-linked carbon fibers and shells. These apparently form as the result of the catalytic action of the platinum particles. Consistent with this analysis is the fact that almost no fibers form under those reaction conditions in which no platinum particles are present (Region III, $T > 960$ K).

ACKNOWLEDGMENT

We gratefully acknowledge the National Science Foundation (Grant CBT-8616502) for providing financial support for this work.

REFERENCES

1. Baker, R. T. K., and Harris, P. S., *in* "Chemistry and Physics of Carbon" (P. L. Walker, Jr. and P. A. Thrower, Eds.), Vol. 14, p. 83. Dekker, New York, 1978.
2. Trimm, D. L., *Catal. Rev. Sci. Eng.* **16,** 155 (1977).
3. Bartholomew, C. M., *Catal. Rev. Sci. Eng.* **24,** 67 (1982).
4. Everett, M. R., Kinsey, D. V., and Romberg, E., *in* "Chemistry and Physics of Carbon" (P. L. Walker, Jr., Ed.), Vol. 3, p. 289. Dekker, New York, 1968.
5. Irving, S. M., and Walker, P. L., Jr., *Carbon* **5,**399 (1967).
6. Presland, A. E. B., and Walker, P. L., Jr., *Carbon* **7,** 1 (1969).
7. Fryer, J. R., and Paal, E., *Carbon* **11,** 665 (1973).
8. Walker, P. L., Jr., and Thomas, J. M., *Carbon* **8,** 103 (1970).
9. Lobo, L. S., and Trimm, D. L., *J. Catal.* **28,** 15 (1973).
10. Yang, K. L., and Yang, R. T., *Carbon* **24,** 687 (1986).
11. Kishimoto, S., Sotani, N., Niimi, K., and Urata, T., *Bull. Chem. Soc. Japan* **51,** 1887 (1978).
12. Wu, N. L., and Phillips, J., *J. Phys. Chem.* **89,** 591 (1985).
13. Wu, N. L., and Phillips, J., *J. Appl. Phys.* **59,** 769 (1986).
14. Holstein, W. L., Moorehead, R. D., Poppa, H., and Boudart, M., *in* "Chemistry and Physics of Carbon," Vol. 18, p. 139. Dekker, New York, 1984.
15. Goresy, A. E. L., and Donnay, G., *Science* **161,** 363 (1968).
16. Vayenas, C. G., Georgakis, C., Michaels, J., and Tormo, J., *J. Catal.* **67,** 348 (1981).
17. Vayenas, C. G., Lee, B., and Michaels, J., *J. Catal.* **66,** 36 (1980).
18. Zuniga, J. E. and Luss, D., *J. Catal.* **53,** 312 (1978).
19. Somorjai, G. A., *Catal. Rev.* **7,** 87 (1972).
20. Pignet, T. P., Schmidt, L. D., and Jarvis, N. L., *J. Catal.* **31,** 145 (1973).
21. Biscoe, J., and Warren, B. E., *J. Appl. Phys.* **13,** 364 (1942).
22. Badami, P. V., Joiner, J. C., and Jones, G. A., *Nature (London)* **215,** 386 (1967).
23. Heimann, R. B., Kleiman, J., and Salansky, N. M., *Carbon* **22,** 147 (1984).
24. Smith, P. P. K., and Buseck, P. R., *Science* **216,** 984 (1982).

25. Baron, K. B., Blakely, D. W., and Somorjai, G. A. *Surf. Sci.* **41,** 45 (1974).
26. Cullis, C. F., Presland, A. E. B., Read, I. A., and Trimm, D. L., "2nd Conference on Industrial Carbon and Graphite," p. 195. Soc. of Chem. Industry, London, 1966.
27. Tesner, P. A., and Refalkes, I. S., *Dokl. Acad. Nauk SSSR* **87,** 821 (1952).
28. Thomas, J. M., *in* "Chemistry and Physics of Carbon" (P. L. Walker, Jr. and P. A. Thomas, Eds.), Vol. 1, p. 121. Dekker, New York, 1966.
29. Boellaard, E., de Bokx, P. K., Koch, A. J. H. M., and Gues, J. W., *J. Catal.* **96,** 481, (1985).
30. Oberlin, A., and Endo, M., *J. Crystallogr. Growth* **32,** 335 (1976).
31. Baker, R. T. K., Yates, D. J. C., and Dumesic, J. A., *in* "Coke Formation on Metal Surfaces" (L. F. Albright and R. T. K. Baker, Eds.), Vol. 202, p. 1. A. C. S. Symposium Series, 1981.
32. Baker, R. T. K., Barber, M. A., Harris, P. S., Feates, F. S., and Waite, R. J., *J. Catal.* **26,** 51 (1972).
33. Rostrup-Nielsen, J., and Trimm, D. C., *J. Catal.* **48,** 155 (1977).
34. Baker, R. T. K., and Waite, R. J., *J. Catal.* **37,**101 (1975).
35. Baird, T., Fryer, J. R., and Grant, B., *Carbon* **12,** 591 (1974).
36. Kock, A. J. H. M., de Bokx, P. K., Boellaard, E., Klop, W., and Geus, J. W., *J. Catal.* **96,** 468 (1985).
37. Lenher, S. *J. Amer. Chem. Soc.* **53,** 3752 (1931).
38. Westbrook, C. K., Dryer, F. L., and Schug, K. P., *in* "Nineteenth Symposium (International) on Combustion," p. 153. The Combustion Institute, Pittsburgh, 1982.
39. Warnatz, J., *in* "Eighteenth Symposium (International) on Combustion," p. 369. The Combustion Institute, Pittsburgh, 1981.
40. Frenklach, M., Ramachandra, M. K., and Matula, R. A., *in* "Twentieth Symposium (International) on Combustion, " p. 871. The Combustion Institute, Pittsburgh, 1984.
41. Aref'evaand, E. F., and Tesner, P. A., *Combust. Explos. Shock Waves* **22,** 326 (1986).
42. Whittaker, A. G., *Science* **200,** 763 (1978).
43. Sladkov, A. M., and Kudryartsev, Yu. P., *Priroda* **58,** 37 (1969).
44. Kasatochkin, V. I., "The Structure Chemistry of Carbon," p. 7. Nanka, Moscow, 1969.
45. Saldkov, A. M., *Sov. Sci. Rev. Sect.* **B 3,** 75 (1981).
46. Haytsu, R., Scott, R. G., Studier, M. H., Lewis, R. S., and Anders, E., *Science* **209,** 1515 (1980).
47. Eastmond, R., Johnson, T. R., and Walton, D. R. M., *Tetrahedron* **28,** 4608 (1972).